

# Detonation propagation in hydrogen–air mixtures with transverse concentration gradients

L. R. Boeck<sup>1</sup>  · F. M. Berger<sup>1</sup> · J. Hasslberger<sup>1</sup> · T. Sattelmayer<sup>1</sup>

Received: 14 July 2014 / Revised: 20 May 2015 / Accepted: 27 August 2015 / Published online: 29 September 2015  
© Springer-Verlag Berlin Heidelberg 2015

**Abstract** The influence of transverse concentration gradients on detonation propagation in H<sub>2</sub>–air mixtures is investigated experimentally in a wide parameter range. Detonation fronts are characterized by means of high-speed shadowgraphy, OH\* imaging, pressure measurements, and soot foils. Steep concentration gradients at low average H<sub>2</sub> concentrations lead to single-headed detonations. A maximum velocity deficit compared to the Chapman–Jouguet velocity of 9 % is observed. Significant amounts of mixture seem to be consumed by turbulent deflagration behind the leading detonation. Wall pressure measurements show high local pressure peaks due to strong transverse waves caused by the concentration gradients. Higher average H<sub>2</sub> concentrations or weaker gradients allow for multi-headed detonation propagation.

**Keywords** Detonation · Hydrogen · Concentration gradient

## 1 Introduction

One major current knowledge gap in hydrogen safety research concerns the influence of mixture inhomogeneity on deflagration and detonation propagation [1, 2]. In real-world accident scenarios, three-dimensional concentration gradients are likely to form. A step toward such scenarios can be made by comparing homogeneous mixtures to such with a

one-dimensional concentration gradient with regard to the propagation characteristics of combustion waves. This work investigates detonations in H<sub>2</sub>–air mixtures with concentration gradients normal to the main direction of detonation propagation.

There have been a number of studies on this topic. Ishii and Kojima [3] examined fuel-lean H<sub>2</sub>–O<sub>2</sub> and H<sub>2</sub>–O<sub>2</sub>–N<sub>2</sub> mixtures with transverse concentration gradients experimentally in a detonation channel of 40 mm height. Relatively weak gradients were used. Local equivalence ratios ranged from about 0.7 to 1 in case of the steepest gradient in H<sub>2</sub>–O<sub>2</sub>. Tilted detonation fronts were observed in schlieren measurements. Soot foils showed detonation cells adapting dynamically to the local mixture composition. The authors furthermore found a velocity deficit of detonations in gradient mixtures compared to homogeneous mixtures. The average equivalence ratio was not kept constant between different gradients which complicates the quantitative interpretation of results.

Ettner et al. [4] performed Euler simulations of detonations in H<sub>2</sub>–air mixtures with transverse gradients. Curved multi-headed detonation fronts with a Mach-stem in the fuel-lean region were observed. The macroscopic detonation front shape remained constant over the propagation distance. Asymmetric wall pressure loads occurred, being highest in the region of lowest fuel concentration due to Mach-stem formation.

Kessler et al. [5] presented simulations in mixtures with varying activation energy and transverse gradients. They found a complex structure of the reaction zone including regions with delayed deflagrative combustion behind the detonation front. A deficit in propagation velocity of about 5–10 % was observed compared to the Chapman–Jouguet velocity  $D_{CJ}$ . This was compared to results by Calhoun and Sinha [6] who computed detonation velocities of about 94 %  $D_{CJ}$  before the gradients caused failure of the

Communicated by N. Smirnov and A. Higgins.

✉ L. R. Boeck  
boeck@td.mw.tum.de

<sup>1</sup> Lehrstuhl für Thermodynamik, Technische Universität München, Boltzmannstr. 15, 85748 Garching, Germany

detonation. Local decoupling of the shock and reaction zone was observed.

As will be shown later, detonations in transverse concentration gradients can exhibit similar characteristics as detonations propagating in two layers of mixture with different reactivities. More literature exist on such configurations. Dabora et al. [7] reported a velocity deficit of detonations in layers of  $H_2$ – $O_2$  bounded by  $N_2$ . A velocity deficit beyond 8–10% led to failure of detonation. Near this limit spinning detonations were observed.

Oran et al. [8] numerically studied detonation transmission in  $H_2$ – $O_2$  from a primary to a secondary mixture. The authors compared their results to experimental work by Liu et al. [9]. Characteristic detonation patterns formed depending on the relative values of the Chapman–Jouguet velocities of the primary and secondary mixtures. Detonations either failed or re-initiated in the secondary mixture. The authors pointed out that the unsteadiness of detonation transmission needs to be considered for predicting the detonation pattern.

Tonello et al. [10] investigated layered  $H_2$ – $O_2$  mixtures experimentally. Similar to the aforementioned studies different types of diffraction patterns were observed depending on the respective reactivities of the primary and secondary mixtures. The detonation velocity in the mixture of higher reactivity was decreased while that in the other mixture was increased.

Lieberman and Shepherd [11] investigated detonation interaction with a diffuse interface between two mixture layers. They concluded that detonation curvature and decoupling of shock and reaction zone may occur, depending on the local mixture dilution.

In a more recent study, Rudy et al. [12] investigated critical conditions of layered  $H_2$ –air detonations in a semi-confined, large-scale experiment. The mixture was bounded by a solid wall on the top and by air on the bottom. For homogeneous layers, a minimum layer height for detonation propagation corresponding to three times the detonation cell size was found. They also examined mixtures with nearly linear transverse concentration gradients. Local concentrations were kept below stoichiometry. The mean  $H_2$  concentration within the detonation layer needed to exceed approximately 16.6 vol% to allow for detonation propagation. Locally, no detonation was observed if the local  $H_2$  concentration was lower than 14 vol%.

Numerical simulations of detonations in layers of generic mixtures were recently presented by Gaathaug et al. [13] with a particular focus on the role of detonation front stability. A critical layer height of about three detonation cells for low activation energy mixtures (moderately stable) was determined. Failure and reinitiation of detonation was observed for high activation energy mixtures (unstable).

In the present work, we investigate a wide range of average  $H_2$  concentrations (22.5–45 vol%) and gradients.

For example, a maximum spread of local  $H_2$  concentration between 10 and 52 vol% can be generated across a concentration gradient in a mixture at 30 vol% average  $H_2$  concentration. This extends the experimental work of Ishii and Kojima [3] toward steeper gradients and toward globally fuel-rich mixtures. In contrast to Rudy et al. [12] we study an entirely confined channel configuration. Results are compared to studies on layered mixtures. Highly time-resolved shadowgraphy,  $OH^*$  imaging and pressure measurements are employed to resolve the detonation front dynamics. Additionally, we use soot foils to gain information on the cellular detonation structure.

## 2 Experimental setup

The explosion channel (Fig. 1) used in the present work has a rectangular cross section (height = 0.06 m and width = 0.3 m). For detonation velocity measurements the channel is composed of six standard segments resulting in a total length of 5.4 m. For optical investigations, one of these segments is replaced by a shorter segment with side-wall quartz windows, thus allowing for taking images of detonations viewing the channel from the side. The resulting field of view covers the channel height of 0.06 m and a width of up to 0.2 m (axial direction of the channel, referred to as the  $x$ -direction in the following). All images presented in this paper are line-of-sight integrated across the 0.3 m channel width. For detonation studies, the viewing window is located at a fixed axial position between  $3.8 \text{ m} < x < 4.0 \text{ m}$ . Only for visualizing the onset of detonation (Fig. 5), the viewing window is shifted to  $2.0 \text{ m} < x < 2.2 \text{ m}$ . The total channel length is 5.1 m when the window section is installed. In both channel configurations, the first section of the channel ( $0.25 \text{ m} < x < 2.05 \text{ m}$ ) contains flat plate obstacles with a blockage ratio of 60% at a spacing of 0.3 m for effective flame acceleration to obtain transition to detonation whereas the second section ( $x > 2.05 \text{ m}$ ) is unobstructed. All experiments are conducted at initial ambient pressure and temperature.

Figure 2a shows the generation of concentration gradients. First, the channel is filled with air at sub-atmospheric pressure. Then,  $H_2$  is injected through the top plate via 153 injection ports (1), a horizontal  $H_2$  layer forms (2) and diffusion occurs (3). The orientation of the resulting gradients (4)

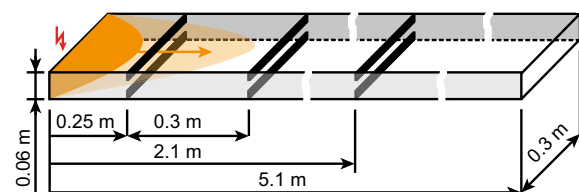
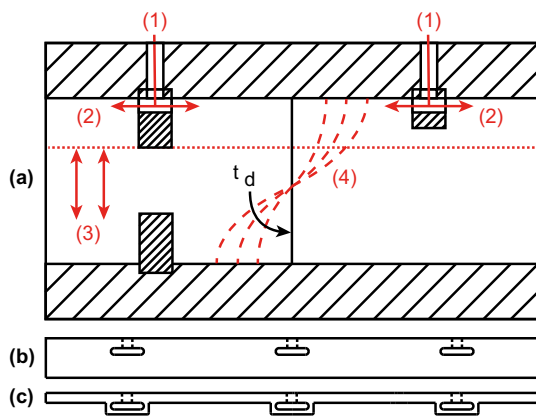


Fig. 1 Experimental setup



**Fig. 2** Mechanism of concentration gradient generation, channel side view (a): injection (1), H<sub>2</sub> layer formation (2), diffusion (3), gradient slope according to diffusion time  $t_d$  (4). Injection through obstacles, view in  $x$ -direction (b). Injection through manifolds, view in  $x$ -direction (c)

is vertical and thus normal to the main direction of detonation propagation. Gradients of defined slope can be generated depending on the diffusion time  $t_d$  between injection and ignition. A diffusion time of 60 s yields a homogeneous mixture, whereas a diffusion time of 3 s results in a steep concentration gradient. Injection ports are distributed as follows: one row of ports comprises three ports along the channel width; the axial spacing between the rows is 0.1 m throughout the entire channel. At obstacle positions in the obstructed channel section, H<sub>2</sub> deflection is achieved by slots in the upper obstacles (Fig. 2b). Positions between the obstacles as well as the unobstructed section are equipped with manifolds protruding into the channel at the upper wall (Fig. 2c). These manifolds do not significantly influence the DDT process as shown in [14, 15]. Likewise, they are not responsible for detonation phenomena observed in this work as will be shown in Sect. 3. Figures 3 and 4 show gradient profiles from CFD simulations [16] taking into account the injection and the diffusion process that are relevant for this work. These simulations were validated against gas chromatography measurements [17, 18]. Simulations and gas chromatography in general show good agreement. In particular, it was proven that a diffusion time of 60 s yields a homogeneous mixture. Differences between simulation and gas chromatography appear in case of the steepest concentration gradients. There, the simulated profiles are steeper than the experimental profiles. This may be caused by non-isokinetic gas probing (quiescent mixture in the channel is sucked into the gas probe volume) and by inaccuracies in the numerical prediction of mixing. In the present work, simulated profiles are used for qualitative comparison of concentration gradients.

The mixture is ignited by an electric spark at  $x = 0$  m after mixture preparation. Piezoelectric pressure transducers (Kistler 601A) in the upper channel wall allow for the determination of overpressure. Average detonation veloc-

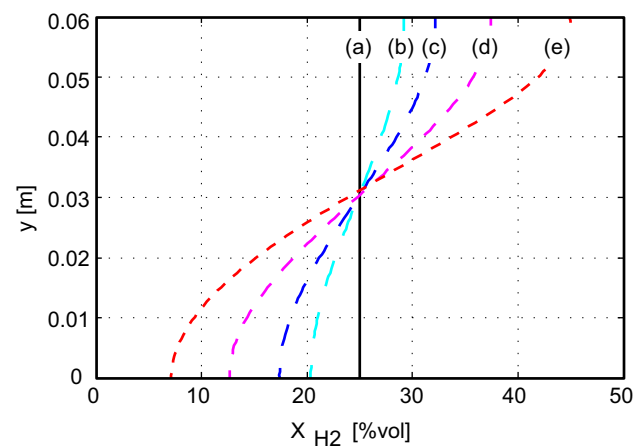


**Fig. 3** Concentration gradient profiles from CFD [16], average H<sub>2</sub> concentration of 25 vol%. Concentration gradients (diffusion times  $t_d$ ): 60 s (a); 10 s (b); 7.5 s (c); 5 s (d); 3 s (e)

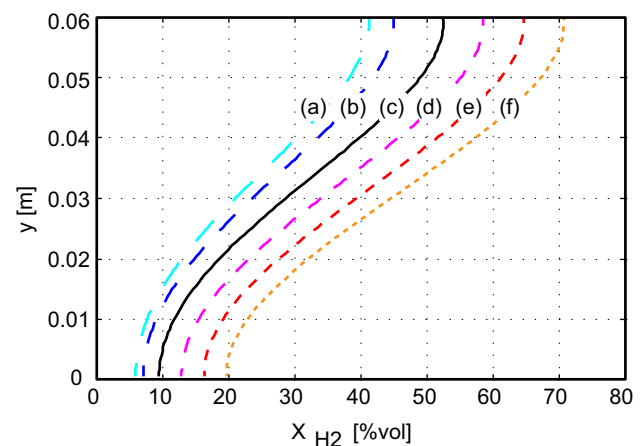


**Fig. 4** Concentration gradient profiles from CFD [16],  $t_d = 3$  s. Average H<sub>2</sub> concentrations: 22.5 vol% (a); 25 vol% (b); 30 vol% (c); 35 vol% (d); 40 vol% (e); 45 vol% (f)

ity is measured by means of pressure transducers  $p_4$  ( $x = 3.2$  m) and  $p_6$  ( $x = 5.0$  m). Shadowgraphy has been found to be most suitable for the optical characterization of detonation fronts. Since the sensitivity of the employed shadowgraph system is very high, no schlieren knife edge is installed. A Photron SA-X high-speed camera is used for shadowgraphy in a classical Z-type mirror setup. Additionally, OH\* luminescence is recorded by combining the camera with a Hamamatsu image intensifier (type C10880-03) and a bandpass filter (central wavelength 307 nm, width 10 nm). These images resolve the location of chemical reaction and hot spots inside the detonation front more clearly. One concave mirror from the shadowgraph system is employed for the OH\* measurements in order to provide a parallel view into the channel and thus avoid perspective distortion of the images. Further details on the experimental setup are provided by Vollmer [18] and Boeck [15].

### 3 Results and discussion

#### 3.1 Onset of detonation

Before presenting detonation experiments, the onset of detonation in the experimental setup is discussed. Particularly for detonation velocity measurements, it is essential that a quasi-steady velocity is reached upstream of the velocity measurement section. Among all average  $H_2$  concentrations and concentration gradients, the case with 22.5 vol% and  $t_d = 3$  s yields the highest run-up distance to onset of detonation. This case will be discussed in the following.

Onset of detonation occurs at the last obstacle of the obstructed channel section,  $x = 2.05$  m, far upstream of the channel sections used for detonation characterization. This obstacle can be seen in Fig. 5. Note that images within this shadowgraph sequence are not equidistant in time. Onset of detonation can be described as a well-known three-step process: first, the fast deflagration precursor shock is reflected at the obstacle. This causes rapid auto-ignition [local explosion, (1)] at the upper obstacle in post-reflected-shock gas, thus in the region of highest local  $H_2$  concentration within the concentration gradient profile. At the lower obstacle,

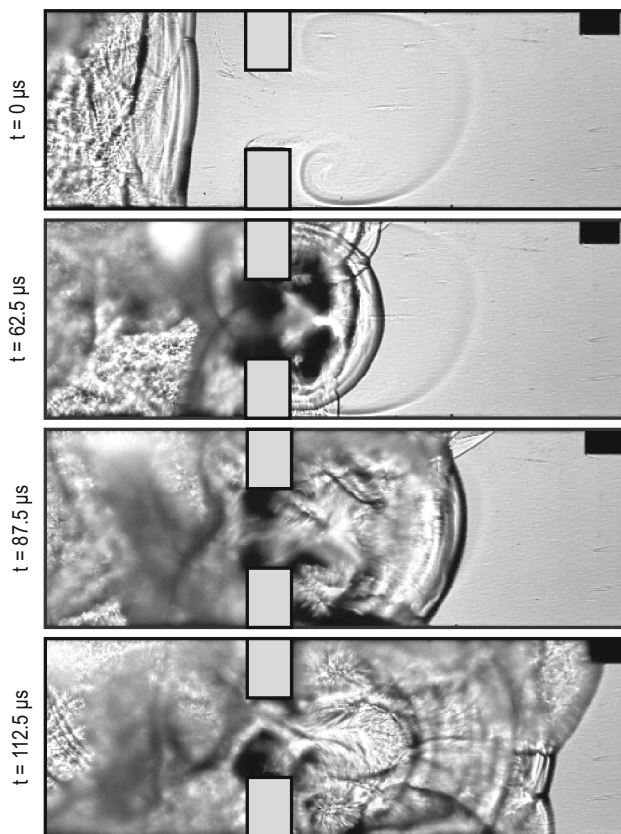


**Fig. 5** Onset of detonation in a 22.5 vol%,  $t_d = 3$  s mixture at the last obstacle,  $x = 2.05$  m

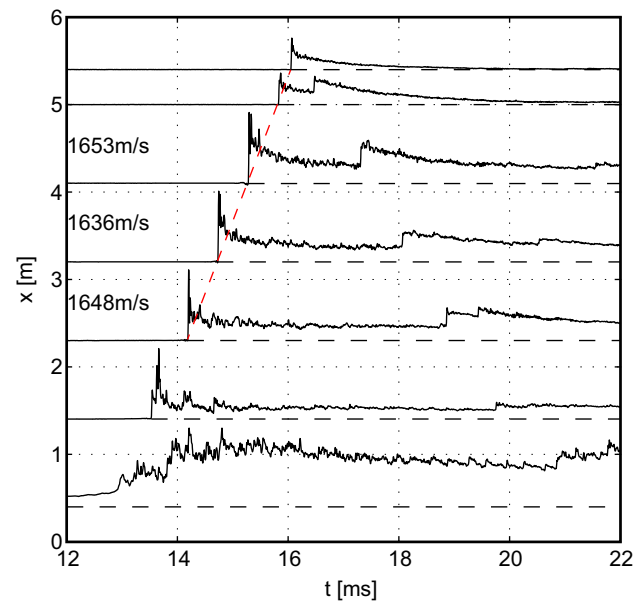


**Fig. 6** Pressure trace diagram, 22.5 vol%,  $t_d = 3$  s

no local explosion is observed due to the low local  $H_2$  concentration (below 10 vol%). The emerging blast wave diffracts around the obstacle (2) and also forms a reinitiation wave propagating upstream. The blast wave and reaction zone decouple in the obstacle opening,  $t = 62.5$  ms. Final initiation of detonation occurs at the upper channel wall downstream of the obstacle through reflection of the blast wave and secondary hot spot generation (3). The detonation can be seen at  $t = 112.5$  ms as a coupled shock reaction zone complex. It will attain a quasi-steady velocity and front topology shortly after the field of view of Fig. 5, cf. Fig. 6.

Two major insights are relevant for our study of detonations further downstream: the onset of detonation occurs directly behind the obstacle. The detonation structure is established quickly. This conclusion is supported by the corresponding pressure trace diagram shown in Fig. 6. Each pressure signal is normalized by its maximum value. Detonation velocity attains a stable value already behind pressure transducer  $p_3$  ( $x = 2.3$  m). Second, the shadowgraph sequence reveals that the detonation propagates into undisturbed, quiescent mixture in the velocity measurement section and also at the location of optical detonation investigations ( $3.8 \text{ m} < x < 4.0$  m). The first two images of the sequence show a vortex behind the obstacle opening which is a marker for the first significant fluid displacement at this location due to the approaching deflagration. Already in the third image the combustion wave catches up with the leading part of this region. The concentration gradient ahead of the detonation thus maintains the initially generated profile in the downstream measurement section.



### 3.2 Detonation in homogeneous mixtures

Experiments in homogeneous mixtures serve as a reference for the subsequent analysis of detonation propagation in mixtures with transverse concentration gradients. The velocity of detonations in homogeneous mixtures, measured with pressure transducers  $p_4$  and  $p_6$ , is shown in Fig. 7,  $t_d = 60$  s. Velocities are close to the Chapman–Jouguet velocity  $D_{CJ}$  of the respective mixtures.

Shadowgraph images, Fig. 8, show the well-known appearance of detonations in homogeneous mixtures with coupled leading shock and reaction zone as well as triple points moving vertically. The richer the mixture, within the range discussed here, the less these triple points emerge in the shadowgraph images. The reaction zone which is visible as a dark area behind the leading shock becomes narrower. This fits the reduction of ignition delay time with an increase of  $H_2$  concentration.

### 3.3 Detonation in mixtures with transverse concentration gradients: an overview

This section provides an overview of detonation propagation phenomena in mixtures with transverse concentration gradients. Detonation velocities are examined first. Afterwards, a series of measurements at a constant average  $H_2$  concentration of 25 vol% with varying concentration gradient slope is presented.

#### 3.3.1 Detonation velocity

Figure 7 shows that detonations in mixtures with concentration gradients ( $t_d < 60$  s) propagate slower than in

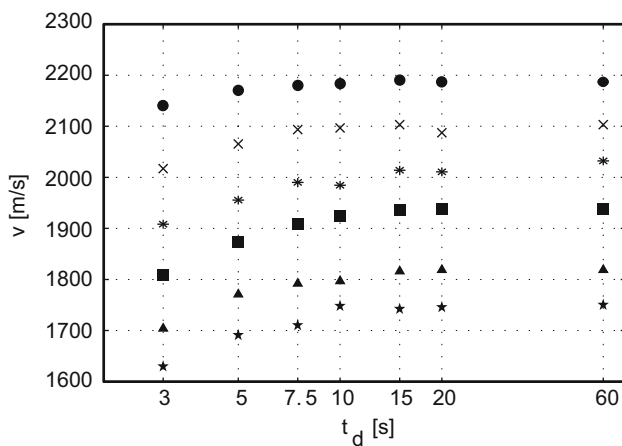


**Fig. 7** Velocities of detonations at different average  $H_2$  concentrations: 22.5 vol% (filled star); 25 vol% (filled triangle); 30 vol% (filled square); 35 vol% (asterisk); 40 vol% (cross); 45 vol% (filled circle). Data points represent average values from five experiments each

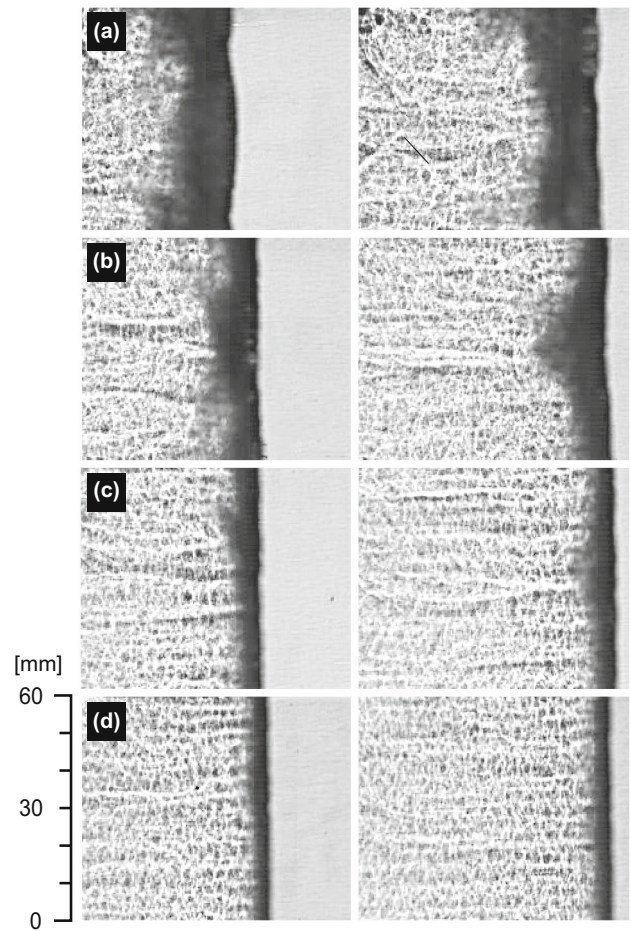


**Fig. 8** Shadowgraph images of detonations in homogeneous mixtures. 12.5  $\mu$ s between images in one row. Average  $H_2$  concentrations: 22.5 vol% (a); 25 vol% (b); 30 vol% (c); 40 vol% (d)

homogeneous mixtures at equal average  $H_2$  concentration. The steeper the gradient, the larger the relative velocity deficit. Mixtures with average concentrations equal to and lower than 30 vol% show similar velocity deficits, while richer mixtures yield smaller deficits. Nevertheless, even the steepest concentration gradients ( $t_d = 3$  s) do not hinder detonation propagation but cause only relatively small velocity deficits up to 9% compared to  $D_{CJ}$  of the mixture, calculated for the average concentration. This value of 9% is in good accordance with the numerical studies by Kessler et al. [5] and Calhoun and Sinha [6]. It was not possible to investigate whether complete failure of detonation can be caused by a concentration gradient in our study because the DDT process in the channel is strongly influenced by the gradient as well [14, 15]. This means that a clear statement if an actual limit for detonation propagation or rather a limit for DDT is observed cannot be reliably made in this type of experiment.

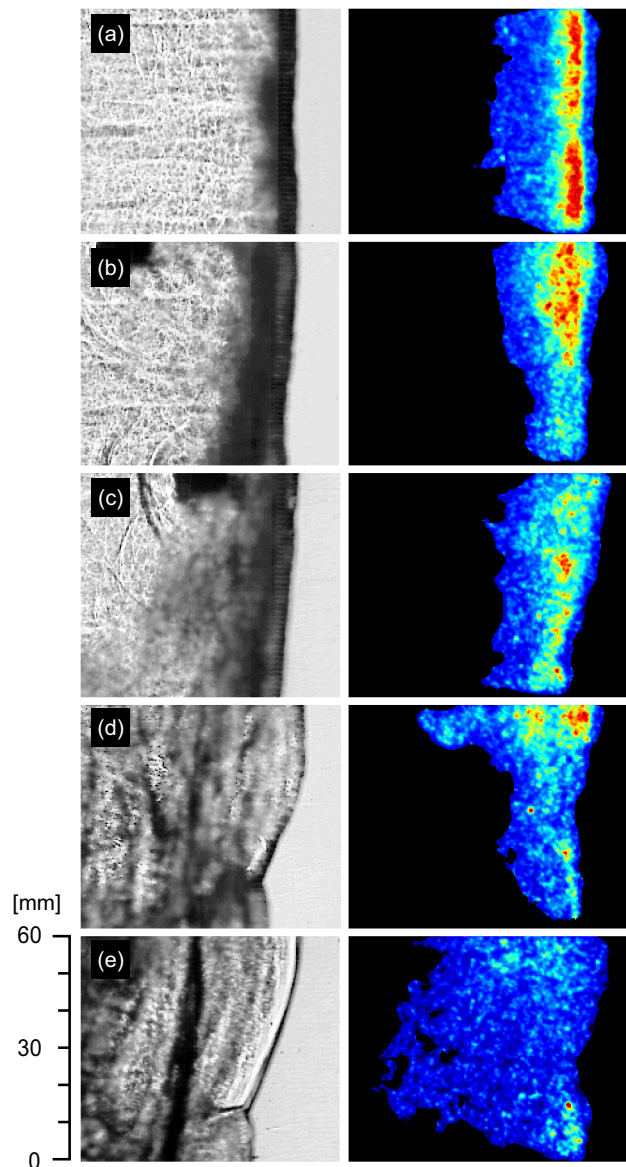


**Fig. 9** Shadowgraph (*left*) and OH\* luminescence (*right*) images of detonation fronts at an average H<sub>2</sub> concentration of 25 vol% at different concentration gradients (diffusion times  $t_d$ ): 60 s (a); 10 s (b); 7.5 s (c); 5 s (d); 3 s (e)

### 3.3.2 Shadowgraph and OH\* images

Figure 9 shows detonation fronts at an average H<sub>2</sub> concentration of 25 vol% and varying gradient slope. Note that shadowgraph and OH\* images were taken in different experiments and thus only show similar, but not identical detonation fronts. The homogeneous mixture (Fig. 9a) allows for multi-headed detonation propagation. Increasing the slope of the concentration gradient, the front gets progressively inclined (Fig. 9b, c). The macroscopic structure of the fronts remains similar to case (a), the fronts are still multi-headed. The highest intensities in the OH\* images appear in the upper region

of the channel due to the higher local H<sub>2</sub> concentrations. The reaction zone widens and becomes more diffuse in the OH\* images.

This regime was also observed by Ishii and Kojima [3]. Gradient profiles in [3] and the present study are not directly comparable due to different mixture composition and gradient shapes. As a first orientation, one may compare the average slope of the concentration gradient in terms of equivalence ratio. The steepest gradient examined in [3] has an average equivalence ratio slope of 0.0075 1/mm, whereas the average gradient slopes for the profiles in Fig. 3 are 0.0065 1/mm (b), 0.011 1/mm (c), 0.019 1/mm (d), and 0.028 1/mm (e). The average gradient slope is thus comparable between experiments in [3] and cases (b) and (c) in the present work.

Between (c) and (d) an obvious change in the propagation mechanism can be observed. One strong single transverse wave appears oscillating across the entire channel height. Following the classical understanding of cellular detonations, there exists only half a detonation cell within the channel height. This regime is subsequently referred to as the single-headed detonation regime. The term single-headed refers to the vertical channel dimension. In the lateral dimension numerous transverse waves must be expected to be present. Typical terminology does not classify the single-headed propagation as a separate regime. However, we want to use this distinction to structure this work due to the pronounced differences that can be observed experimentally.

In the following section, single-headed propagation is described. We focus on the steepest gradients examined ( $t_d = 3$  s). Afterwards, aspects of multi-headed propagation and the transition between the regimes are discussed.

## 3.4 Detonation in mixtures with transverse concentration gradients: single-headed propagation

### 3.4.1 Shadowgraph images

At an average H<sub>2</sub> concentration of 25 vol%,  $t_d = 3$  s, a highly dynamic detonation propagation behavior can be observed. Figure 10 shows shadowgraph images taken at 80,000 frames per second. Two parts of a characteristic cycle can be seen, recorded in two experiments (two columns). This cycle occurs in most of the experiments at average concentrations up to 30 vol% at  $t_d = 3$  s. The structure of the detonation front resembles a single-headed detonation in homogeneous mixtures. One strong transverse wave forms which is periodically reflected off the channel walls. Comparable to the formation of transverse waves in homogeneous mixtures, this wave forms in order to equilibrate the pressure differences behind the leading detonation front, which are intensified by the hydrogen concentration gradient here.

Reflection of this transverse wave at the channel top causes hot spots that allow for rapid chemical reaction (referred to



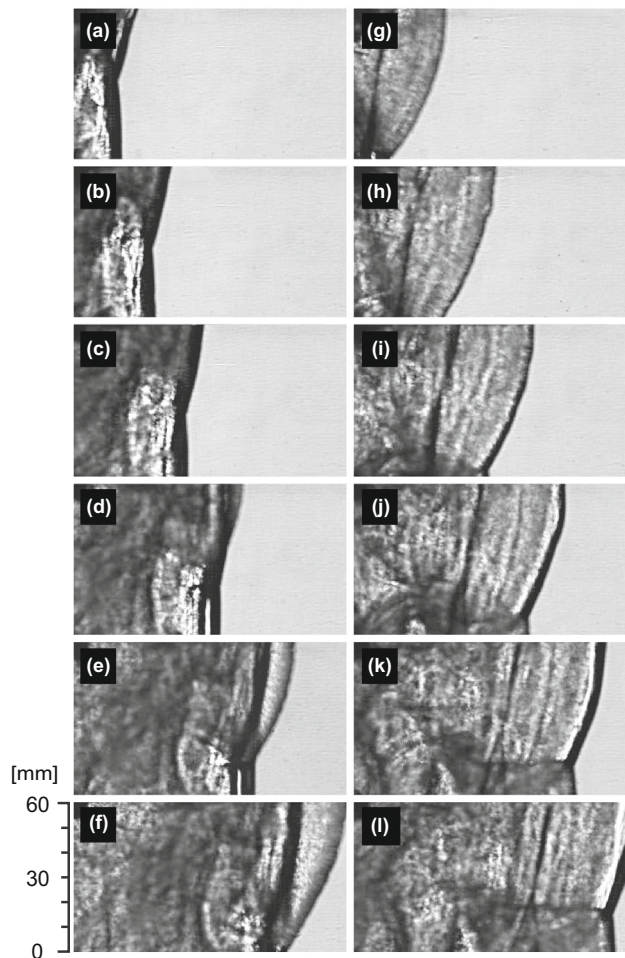


**Fig. 10** Shadowgraph images of detonations at an average  $H_2$  concentration of 25 vol% and  $t_d = 3$  s. The *two columns* represent two experiments.  $12.5 \mu\text{s}$  between images in one column

as a local explosion in the following) and thereby periodic re-initiation of detonation. Note that there is no injection manifold installed near the location of the local explosion. Thus, the single-headed regime is clearly not caused by the manifolds but by the concentration gradient itself. Reaction is coupled with the shock within the first frames after transverse wave reflection (Fig. 10a–f). When this wave is reflected off the channel bottom, the reaction is still coupled behind the Mach-stem but gradually decouples behind the incident shock (Fig. 10i–l). Arriving at the channel top, the reflection of the transverse wave again causes a local explosion. This completes one cycle. Local detonation front velocity varies between approximately 1.2 and 0.8 times the average propagation velocity. The gray blurred area, identified as the reaction zone, extends over the entire shadowgraph image. Thus, we assume that significant portions of the mixture react in unburnt pockets as a turbulent deflagration downstream of the leading detonation.

### 3.4.2 $OH^*$ images

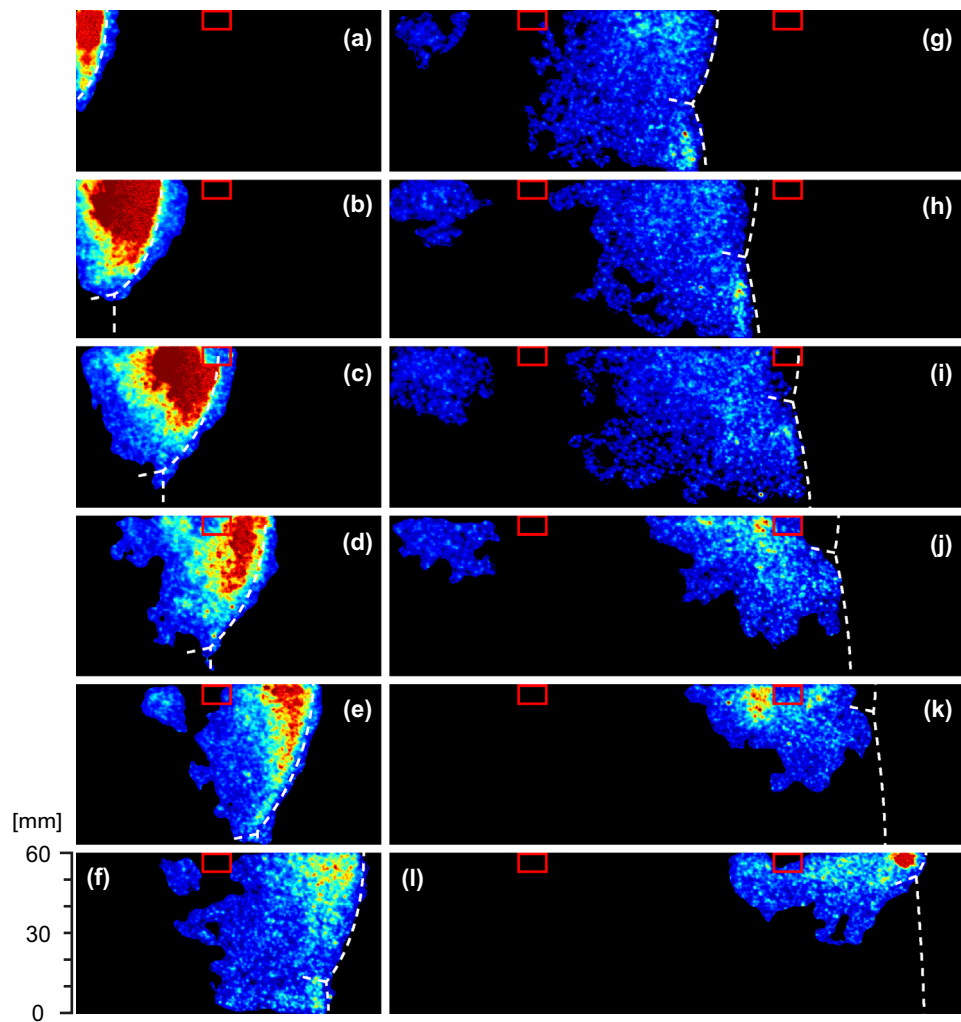
$OH^*$  imaging is useful to distinguish between local explosions, regular detonations and deflagrations.  $OH^*$  images show local explosions as bright spots at a distinctly higher luminosity as compared to the reaction zone behind a detonation at CJ conditions. Deflagrations appear at a lower luminosity than CJ detonations. Following the argumentation of Fiala and Sattelmayer [19], these differences can be attributed to the distinctly higher thermal production rate of electronically excited OH radicals ( $OH^*$ ) at higher temperatures. The thermal production rate is exponentially dependent on temperature in a wide range, while the chemical excitation remains fairly constant at a given pressure.

The  $OH^*$  images in Fig. 11 show one entire cycle as described before. Red rectangles mark the positions of the injection manifolds. Beginning with the strong local explosion at the channel top—clearly upstream of the manifold—with a high local luminescence in Fig. 11a, the overdriven explosion front propagates toward the channel bottom (Fig. 11a–e). The front interacts with the manifold in Fig. 11c, but no influence on the overall propagation mechanism can be seen. As the propagation velocity of the expanding front decreases, the luminosity decreases accordingly. Enhanced reaction behind the Mach-stem after reflection of the transverse wave at the bottom wall can be clearly seen (Fig. 11f). Figure 11f–l comprises the upward propagation phase. As the shadowgraph images already showed, decoupling of shock and reaction zone occurs in the upper channel region. The luminosity decreases sharply and the separation distance between the assumed shock front, reconstructed from shadowgraph images, and the reaction zone increases at the channel top. Behind the Mach-stem the images show no further significant reaction toward the end of the cycle. In Fig. 11j the front interacts with the second manifold in the field of view. Reflection at the manifold causes elevated luminescence due to locally increased temperature, but a local explosion is not observed. In the last frame (Fig. 11l), reflection of the transverse wave at the channel top triggers the volumetric explosion of the precompressed, unburnt mixture pocket between incident shock and decoupled reaction zone. Detonation is thereby re-initiated and the next cycle begins. This image sequence furthermore shows that only about half the propagation cycle seems to be driven by shock-induced auto-ignition. A significant share of the mixture seems to be consumed rather by deflagration than through auto-ignition.

### 3.4.3 Soot foils

Soot foil measurements were performed to see if traces at the channel side walls confirm the previous observations. This is especially important since the channel width is large (0.3 m),

**Fig. 11** OH\* luminescence images of a detonation at an average H<sub>2</sub> concentration of 25 vol% and  $t_d = 3$  s. 12.5  $\mu$ s between images



which means that the line-of-sight integration inherent to shadowgraphy and OH\* imaging may lead to doubtful conclusions. Sooted plates were therefore installed at the window section position. Clear imprints on these sooted plates were obtained at an average H<sub>2</sub> concentration of 30 vol%. Results are presented in Fig. 12. The soot foil gained from a homogeneous mixture (Fig. 12a) serves as a reference. One cycle of transverse wave oscillation was captured on one soot plate in the 30 vol% mixture at  $t_d = 3$ , (Fig. 12b). A shallow upward-leading trajectory corresponds to the triple point formed by incident shock, Mach-stem and upward-propagating transverse wave. The transverse wave propagates slowly in this part of the cycle compared to the incident shock. The steep downward-leading trajectory corresponds to the triple point after local explosion at the channel top. The arrow in Fig. 12b highlights the location of the local explosion. The soot foil can furthermore be used to ensure that the injection manifolds do not cause the single-headed regime. From the foil, the cycle length can be estimated at about 0.18 m, not being related to the manifold spacing of 0.1 m. A second transverse

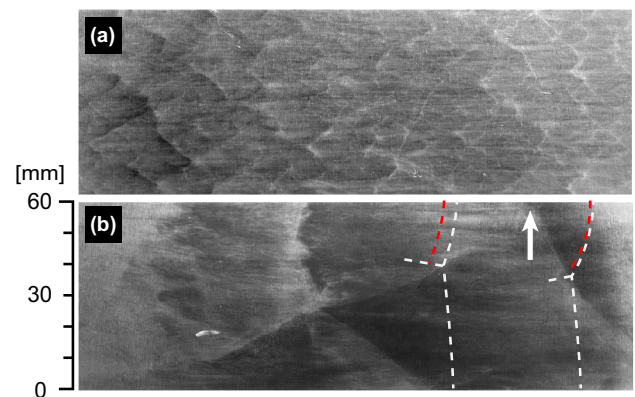
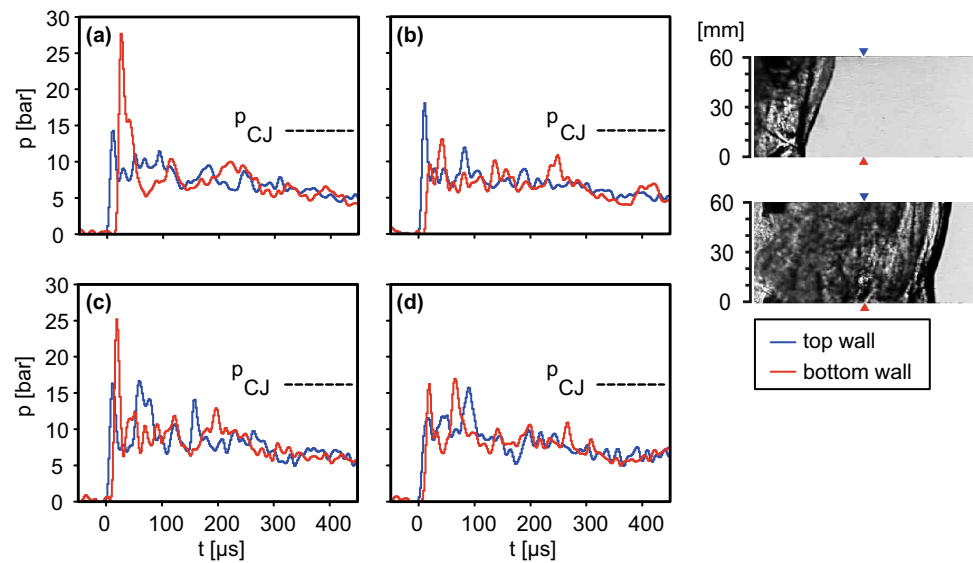


**Fig. 12** Soot foils of detonations at an average H<sub>2</sub> concentration of 30 vol%.  $t_d = 60$  s (a);  $t_d = 3$  s (b)

wave may be visible on this plate, but the interaction with transverse waves moving in the spanwise direction of the channel, which is visible as vertical wavy imprints on the plate, complicates the analysis.



**Fig. 13** Overpressure at the upper and lower channel walls at  $t_d = 3$  s and different average  $H_2$  concentrations: 22.5 vol% (a, b), 30 vol% (c, d); Shadowgraph images for case (a). Triangles show the pressure transducer positions



### 3.4.4 Pressure measurements

Single-headed detonations were further examined by wall pressure measurements. The window segment was equipped with two facing pressure transducers, one in the top plate and one in the bottom plate. Figure 13 shows measurements at 22.5 vol% (a, b) and 30 vol% (c, d) average  $H_2$  concentration at  $t_d = 3$  s. The detonation generally arrives at the upper transducer first due to its curved shape. High local peak overpressure well beyond CJ values can be caused by the strong transverse wave which is periodically reflected off the channel walls. In Fig. 13a, c it is reflected at the bottom wall in close vicinity of the pressure transducer. Figure 13, far right, shows shadowgraph images recorded simultaneously with the pressure measurement of case (a). The triangles mark the positions of the pressure transducers. Between these two images, reflection at the bottom wall occurs, yielding high peak overpressure in the range of two times CJ pressure. On the other hand, Fig. 13b, d shows experiments where the transverse wave is not reflected close to either of the transducers, resulting in peak overpressures close to CJ pressure. Measured peak overpressure thus primarily depends on the location of pressure measurement relative to the location of transverse wave reflection. Pressure differences between the upper and lower wall equilibrate quickly behind the leading front, typically within one transverse wave oscillation period.

### 3.5 Detonation in mixtures with transverse concentration gradients: multi-headed propagation

In mixtures richer than 35 vol% at  $t_d = 3$  s, detonation propagation is multi-headed. Transverse waves are continuously regenerated by collisions with oncoming transverse waves and with the channel walls. If enough transverse waves exist,

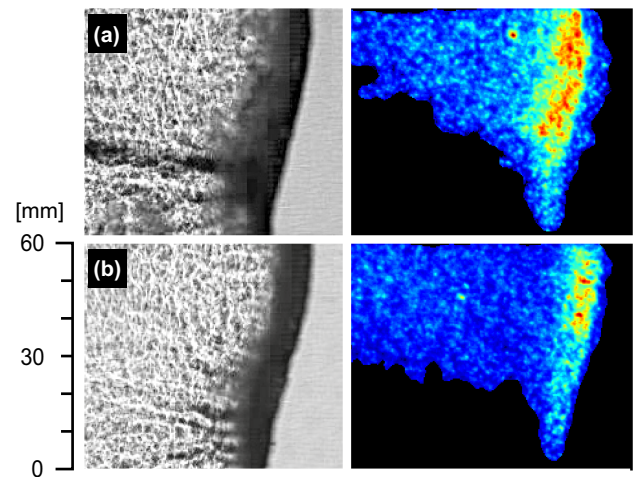


**Fig. 14** Shadowgraph (left) and  $OH^*$  (right) images of detonation fronts at  $t_d = 3$  s at different average  $H_2$  concentrations: 35 vol% (a); 40 vol% (b)

solid walls on both sides are not necessarily required for detonation propagation—in contrast to the single-headed regime which depends on periodic wall reflections. This regime equivalently appears in leaner mixtures with weaker gradients as shown in Fig. 9a–c. Figure 14 shows detonation fronts in 35 vol% (a) and 40 vol% (b)  $H_2$  at  $t_d = 3$  s. The major difference from lower average  $H_2$  concentrations is a constant front curvature over time without visible Mach-stem formation. The reaction zone (dark zone in shadowgraph images) is much narrower. This indicates a higher portion of mixture being directly consumed by auto-ignition, which may be an explanation for the lower velocity deficit of such detonations compared to single-headed detonations. A strong transverse wave like in Fig. 10 does not form. Soot foil measurements (Fig. 15b) show curved traces similar to the observations of

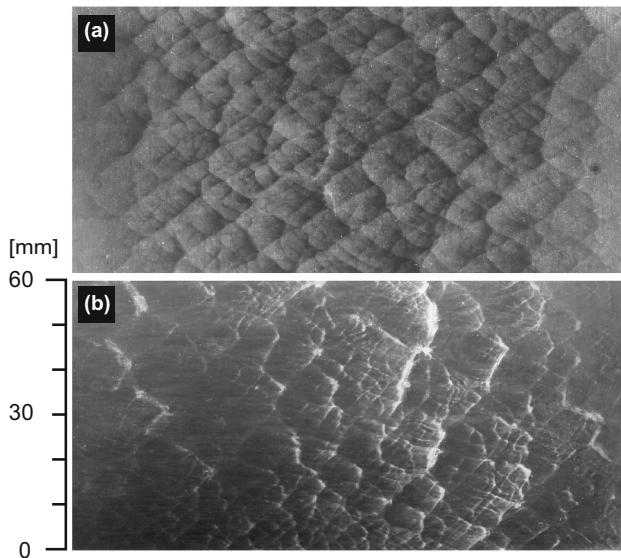


**Fig. 15** Soot foils of detonations at an average  $H_2$  concentration of 40 vol%.  $t_d = 60$  s (a);  $t_d = 3$  s (b)

Ishii and Kojima [3]. Detonation cells are asymmetric compared to the pattern in the homogeneous mixture (Fig. 15a) with a higher degree of substructures. Near the walls, large cells would be expected, taking into account the respective local  $H_2$  concentrations. It is thus surprising that cells remain very small even far away from the channel center line.

### 3.6 Detonation in mixtures with transverse concentration gradients: the transition between propagation regimes

Two detonation regimes were observed experimentally: single-headed propagation with one strong transverse wave and multi-headed propagation with a constant macroscopic front curvature over time and numerous weak transverse waves. The single-headed regime can be interpreted as a near-limit phenomenon similar to the spinning detonation observed by Dabora et al. [7]. It is also comparable to detonations in mixtures with high activation energy discussed by Gaathaug et al. [13]. The channel height of 0.06 m allows for detonation propagation in homogeneous mixtures with an  $H_2$  concentration down to 16–17 vol%. Single-headed propagation already occurs in mixtures with gradients at significantly higher average  $H_2$  concentrations. It was induced by either steepening the gradient at constant average  $H_2$  concentration or by decreasing the average  $H_2$  concentration while maintaining the gradient slope (within the experimental limitations by keeping  $t_d$  constant).

Detonation cell size data from [20] are used subsequently to interpret the examined concentration gradient profiles with regard to their local mixture reactivity. Calculated local cell sizes cannot directly be expected in reality since the dynamics

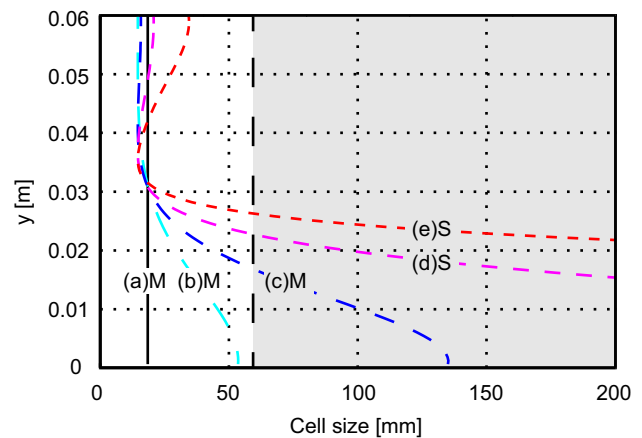


**Fig. 16** Cell size profiles corresponding to Fig. 3, average  $H_2$  concentration of 25 vol%. Concentration gradients (diffusion times  $t_d$ ): 60 s (a); 10 s (b); 7.5 s (c); 5 s (d); 3 s (e)

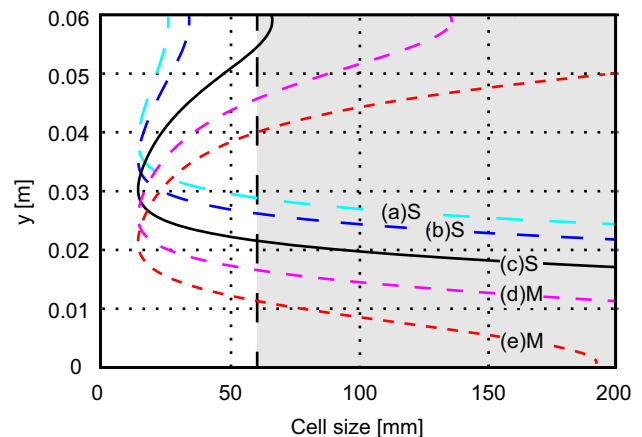


**Fig. 17** Cell size profiles corresponding to Fig. 4,  $t_d = 3$  s. Average  $H_2$  concentrations: 22.5 vol% (a); 25 vol% (b); 30 vol% (c); 35 vol% (d); 40 vol% (e)

of transverse waves not only depends on local conditions, but on the entire oscillation cycle of transverse waves between the channel walls. Figures 16 and 17 provide an analysis of detonation cell size as a function of local  $H_2$  concentration corresponding to the optically characterized concentration gradient profiles in Figs. 3 and 4, respectively.

In case of a constant average  $H_2$  concentration of 25 vol%, Fig. 16, it can be seen that the non-linear dependency between local  $H_2$  concentration and cell size and the strong increase in cell size toward low local  $H_2$  concentrations causes a sharp transition from small cells in the upper channel region to cells distinctly larger than the channel height in the lower part of most gradient profiles. Differences in cell size at the channel top are comparably small. Cases where single-headed propagation occurred, marked with “S”, show the strongest increase in cell size toward the bottom as compared to multi-headed detonations, “M”. This suggests that single-headed propagation occurs as soon as the minimum concentrations

in the lower channel region reach sufficiently low values, causing a sharp increase in local detonation cell size.

An evident qualitative similarity between the first group of experiments, Fig. 16, to detonation propagation in flat layers is the sharp increase in cell size in the fuel-lean region at the channel bottom. Thus, a question is whether an effective detonable layer height required for multi-headed propagation can be defined. For semi-confined configurations with homogeneous mixtures, a layer thickness of about three times the cell size is required for self-sustained multi-headed detonation propagation. The required number of detonation cells might be lower in the entirely confined configuration because reflection of transverse waves at the lower wall supports detonation propagation. For the following analysis only cells smaller than the channel height of 0.06 m are considered since this would pose the lower limit for detonation propagation in a homogeneous mixture.

Table 1 shows the overall height within the channel where cells are smaller than the channel height, referred to as the detonable layer height in the following, and the average cell size in this region. Cases with single-headed detonations show detonable layer heights lower than 40 mm with less than two cells of average size in this region. Transition from single- to multi-headed detonation occurs when the detonable layer height exceeds about 40 mm. This corresponds to about two detonation cells being present in the detonable region. This value is close to the critical layer height of three cells found by Rudy et al. [12] and Gaathaug et al. [13]. While detonation fails in thinner layers in semi-confined configurations, the entirely confined channel in the present work still allows for detonation propagation in the single-headed regime.

Detonation cell size profiles in Fig. 17 refer to experiments with steep gradients ( $t_d = 3$  s) at varying average  $H_2$  concen-

tration, cf. Fig. 4. Table 2 shows the corresponding analysis of detonable layer height and average cell size. Cases with single-headed detonations show a detonable layer height of about 30 mm with about 1–1.5 detonation cells of average size in this region. Cell size increases sharply toward the fuel-lean region. In contrast to the profiles in Fig. 16, high average concentrations and steep gradients cause regions of large cells also at the channel top, in particular at average  $H_2$  concentrations of 35 and 40 vol%. Despite this increase in cell size in the fuel-rich region, these two cases allow for multi-headed, stable detonation propagation, cf. Fig. 14. Detonable layer height is again close to 30 mm. Only about one cell of average size is present in this region. The theoretical analysis of local cell size obviously does not deliver useful information on the detonation propagation mechanism in these two cases with globally fuel-rich mixtures.

## 4 Conclusions

The present paper investigated detonation propagation in  $H_2$ –air mixtures with transverse concentration gradients in an entirely closed rectangular channel at laboratory scale. It was shown that even steep gradients do not hinder detonation propagation. Concentration gradients cause a deficit in propagation velocity compared to homogeneous mixtures at equal average  $H_2$  concentration.

The observed detonations were divided into two groups: single-headed detonations with one strong transverse wave and multi-headed detonations with a constant macroscopic front curvature. In single-headed detonations reflection of the transverse wave at the top plate of the channel—in the most fuel-rich region—leads to local explosions, which periodically re-initiate the detonation. Distinct decoupling of shock and reaction zone occurs during each cycle of transverse wave oscillation between the channel walls. The formation of unreacted pockets was observed in  $OH^*$  images. Large amounts of mixture seem to burn as a deflagration behind the leading detonation front. Overpressure measurements at the upper and lower channel walls showed that reflection of the transverse wave locally causes high peak pressures.

Interpreting concentration gradient profiles in terms of local detonation cell sizes seems to provide a useful tool to predict the propagation regime of detonations in globally fuel-lean mixtures with transverse concentration gradients. Cell sizes of the investigated steep gradients increase sharply toward low local  $H_2$  concentrations at the channel bottom. This poses a similarity to layers of reactive mixture bounded by an inert gas or a mixture of distinctly lower reactivity. We defined the detonable layer height, a theoretical parameter, as the region where detonation cells are smaller than the channel height. According to our experiments, about two detonation cells need to be present in the detonable layer to

**Table 1** Average cell size and detonable height for profiles in Fig. 3

Fig. (case)	Avg. cell size (mm)	Detonable height (mm)
Fig. 3 (a)	18.5	60.0
Fig. 3 (b)	26.2	60.0
Fig. 3 (c)	21.6	43.8
Fig. 3 (d)	21.1	37.8
Fig. 3 (e)	25.3	34.2

**Table 2** Average cell size and detonable height for profiles in Fig. 4

Fig. (case)	Avg. cell size (mm)	Detonable height (mm)
Fig. 4 (a)	22.2	31.2
Fig. 4 (b)	25.8	34.2
Fig. 4 (c)	30.3	33
Fig. 4 (d)	28.1	28.8
Fig. 4 (e)	28.2	28.9



allow for multi-headed detonation propagation. If the detonable height is lower, single-headed, unstable detonations occur. By further reducing the detonable layer height by even steeper transverse concentration gradients, failure of detonation will presumably occur. This could however not be investigated in the present experiment. In globally fuel-rich mixtures an increase in cell size also occurs at the channel top. Such profiles are not comparable to a layer of reactive mixture anymore. Multi-headed, very stable detonation propagation is possible even if the theoretically determined detonable region is rather narrow. Scaling experiments in channels of different geometrical sizes are required as a next step to characterize detonation dynamics in mixtures with transverse concentration gradients.

**Acknowledgments** The presented work is funded by the German Federal Ministry of Economic Affairs and Energy (BMWi) on the basis of a decision by the German Bundestag (Project Nos. 1501338 and 1501425) which is gratefully acknowledged.

## References

- Kotchourko, A.: Hydrogen safety research priorities. In: International Conference on Hydrogen Safety (ICHS), Brussels, (2013)
- Breitung, W., Chan, C.K., Dorofeev, S.B., Eder, A., Gerland, B., Heitsch, M., Klein, R., Malliakos, A., Shepherd, J.E., Studer, E., Thibault, P.: Flame acceleration and deflagration-to-detonation transition in nuclear safety. Technical report, OECD State-of-the-Art Report by a Group of Experts, NEA/CSNI/R(2000)7, (2000)
- Ishii, K., Kojima, M.: Behavior of detonation propagation in mixtures with concentration gradients. *Shock Waves* **17**, 95–102 (2007)
- Ettner, F., Vollmer, K.G., Sattelmayer, T.: Mach reflection in detonations propagating through a gas with a concentration gradient. *Shock Waves* **23**, 201–206 (2012)
- Kessler, D., Gamezo, V., Oran, E.: Gas-phase detonation propagation in mixture composition gradients. *Philos. Trans. R. Soc. A* **370**, 567–596 (2012)
- Calhoon, W.H., Sinha, N.: Detonation wave propagation in concentration gradients. In: Proc. 43rd AIAA Aerospace Sciences Meeting and Exhibit, Reno, Nevada (2005)
- Dabora, E.K., Nicholls, J.A., Morrison, R.B.: The influence of a compressible boundary on the propagation of gaseous detonations. In: Symposium (International) on Combustion, vol. 10, pp. 817–830. Elsevier (1965)
- Oran, E.S., Jones, D., Sichel, M.: Numerical simulations of detonation transmission. *Proc. R. Soc. A* **436**, 267–297 (1992)
- Liu, J.C., Sichel, M., Kaufmann, C.W.: The lateral interaction of detonating and detonable gaseous mixtures. *Prog. Astronaut. Aeronaut.* **114**, 264–283 (1988)
- Tonello, N.A., Sichel, M., Kaufmann, C.W.: Mechanisms of detonation transmission in layered H<sub>2</sub>–O<sub>2</sub> mixtures. *Shock Waves* **5**, 225–238 (1995)
- Lieberman, D.H., Shepherd, J.E.: Detonation interaction with a diffuse interface and subsequent chemical reaction. *Shock Waves* **16**, 421–429 (2007)
- Rudy, W., Kuznetsov, M.S., Porowski, R., Teodorczyk, A., Grune, J., Sempert, K.: Critical conditions of hydrogen-air detonation in partially confined geometry. *Proc. Combust. Inst.* **34**, 1965–1972 (2013)
- Gaathaug, A.V., Vaagsaether, K., Bjerketvedt, D.: Detonation propagation in a reactive layer: the role of detonation front stability. In: Proceedings of the 10th International Symposium on Hazards, Prevention and Mitigation of Industrial Explosions, Bergen, Norway (2014)
- Boeck, L.R., Msalmi, M., Koehler, F., Hasslberger, J., Sattelmayer, T.: Criteria for DDT in hydrogen-air mixtures with concentration gradients. In: 10th International Symposium on Hazards, Prevention and Mitigation of Industrial Explosions, Bergen, Norway (2014)
- Boeck, L.R.: Deflagration-to-detonation transition and detonation propagation in H<sub>2</sub>-air mixtures with transverse concentration gradients. PhD thesis. Lehrstuhl für Thermodynamik, Technische Universität München (2015)
- Ettner, F.: Effiziente Numerische Simulation des Deflagrations-Detonations-Übergangs. PhD Thesis, Technische Universität München (2013)
- Vollmer, K.G., Ettner, F., Sattelmayer, T.: Deflagration-to-detonation transition in hydrogen-air mixtures with a concentration gradient. *Combust. Sci. Technol.* **184**, 1903–1915 (2012)
- Vollmer, K.G.: Einfluss von Mischungsgradienten auf die Flammenbeschleunigung und die Detonation in Kanälen. PhD Thesis, Lehrstuhl für Thermodynamik, Technische Universität München (2015)
- Fiala, T., Sattelmayer, T.: A posteriori computation of OH\* radiation from numerical simulations in rocket combustion chambers. In: 5th European Conference for Aeronautics and Space Sciences (EUCASS), Munich, (2013)
- Kaneshige, M., Shepherd, J.E.: Detonation database. Technical Report FM97-8, GALCIT (1997)